## HIGH TEMPERATURE TENSILE PROPERTIES AND DEFORMATION BEHAVIOR OF V-4Cr-4Ti — A. F. Rowcliffe, D. T. Hoelzer, and S. J. Zinkle (Oak Ridge National Laboratory)

### OBJECTIVE

The objective of this work is to determine the strain-rate sensitivity of the tensile properties of V-4Cr-4Ti as a function of temperature over the range RT to 800°C.

### SUMMARY

The tensile deformation behavior of V-4Cr-4Ti has been determined over the range 20 to 800°C for strain rates in the range $10^{-1}$/s to $10^{-5}$/s. Changes in the strain rate sensitivity of stress parameters are linked to the existence of three different regimes of deformation, namely, Lüders extension, dislocation glide/strain hardening, and dislocation creep.

### PROGRESS AND STATUS

Introduction

The work described here is a continuation of an investigation into the strain rate sensitivity of the deformation behavior of the 500 kg-heat of V-4Cr-4Ti (No. 832665). In an initial study [1], the hardening strain rate sensitivity, m, was determined at room temperature for the 500-kg heat and also for the 30-kg heat of V-3Cr-3Ti and V-6Cr-6Ti, where m is defined as

$$m=\frac{1}{\sigma}\frac{\partial\sigma}{\partial \ln\dot{\varepsilon}}\bigg|_{\varepsilon,T} \qquad (1)$$

where $\sigma$ is the stress and $\dot{\varepsilon}$ is the strain rate. It was found that for all three materials, m fell in the range 0.022 to 0.024, which agrees well with the value of 0.024 for pure vanadium (containing 265 wppm oxygen) reported by Bradford and Carlson [2]. Dynamic strain aging (DSA) was observed for all three alloys in the 400 to 700°C regime at a strain rate of $10^{-3}$/s. Later work extended the range of strain rates from $10^{-1}$/s to $10^{-5}$/s and it was shown that a regime of negative strain-rate sensitivity associated with DSA extended down to 300°C in the V-4Cr-4Ti alloy [3]. Measurements of m for V-4Cr-4Ti irradiated in various reactors at temperatures ranging from 200 to 500°C were reported [4] and the radiation-induced changes in m were discussed in terms of a weakly positive component introduced by a high number density of defect clusters. Unirradiated tensile data generated in these studies were presented and combined with data obtained at other laboratories to derive equations describing the temperature dependence of strength and ductility properties at a strain rate of ~$10^{-3}$/s [5]. In this report, new experimental data and the strain rate sensitivities of several stress parameters are discussed in terms of related deformation mechanisms.

Experimental Procedure

Tensile measurements were performed on type SS-3 specimens (nominal gage dimensions 0.76 × 1.52 × 7.6 mm). The specimens used were from the RC/RD series that were prepared from heat no. 832665 using the fabrication steps shown in Table 1. As reported earlier [6], this procedure resulted in a uniform microstructure with an average grain size of ~23 μm and a hardness of 137 DPH after the final anneal at 1000°C for two hours. Testing was carried out under a vacuum of

Table 1. Temperature and Strain Rate Dependence of RD, RC Series Tensile Properties

| Specimen ID | Test Temp. °C | Strain Rate $S^{-1}$ | Initial Yield Stress $\sigma_i$ MPa | Lower Yield Stress $\sigma_y$ MPa | Ultimate Stress $\sigma_u$ MPa | Stress for 8% Strain $\sigma_r$ | Luders Strain $\varepsilon_L$ % | Uniform Strain $\varepsilon_u$ % | Total Strain $\varepsilon_t$ % |
|---|---|---|---|---|---|---|---|---|---|
| Ann. 1000°C, 2h | | | | | | | | | |
| RD16 | RT | $10^{-3}$ | 354 | 335 | 429 | 412 | 0.8 | 15.7 | 30.0 |
| RD13 | 200 | $10^{-3}$ | 259 | 259 | 350 | 338 | 1.2 | 14.8 | 23.8 |
| RC03 | 300 | $10^{-1}$ | 283 | 330 | 349 | 346 | 0.5 | 11.7 | 22.3 |
| RC16 | 300 | $10^{-2}$ | — | 271 | 332 | 330 | — | 13.5 | 22.3 |
| RC02 | 300 | $10^{-3}$ | 212 | 233 | 345 | 326 | 0.8 | 15.0 | 22.7 |
| RC11 | 300 | $10^{-4}$ | 175 | 228 | 346 | 327 | 0.7 | 15.4 | 22.5 |
| RC12 | 300 | $10^{-5}$ | 190 | 220 | 367 | 342 | 0.7 | 19.2 | 26.0 |
| RD04 | 300 | $10^{-5}$ | 175 | 217 | 365 | 350 | 0.4 | 11.9 | 18.0 |
| RC08 | 400 | $10^{-1}$ | 204 | 234 | 330 | 320 | 0.8 | 12.7 | 21.1 |
| RC07 | 400 | $10^{-3}$ | 179 | 214 | 353 | 330 | 0.5 | 16.3 | 23.0 |
| RC04 | 400 | $10^{-3}$ | 198 | 220 | 351 | 330 | 0.8 | 16.5 | 23.0 |
| RC13 | 400 | $10^{-5}$ | 196 | 224 | 375 | 356 | 0.6 | 16.3 | 21.9 |
| RC09 | 500 | $10^{-1}$ | 187 | 230 | 337 | 323 | 0.5 | 15.0 | 22.9 |
| RC05 | 500 | $10^{-3}$ | 225 | 225 | 365 | 342 | 0.9 | 17.7 | 24.0 |
| RD01 | 500 | $10^{-3}$ | 221 | 221 | 366 | 347 | 0.8 | 17.1 | 24.2 |
| RD22* | 500 | $10^{-3}$ | 209 | 220 | 400 | 378 | 0.3 | 14.6 | 22.1 |
| RD05 | 500 | $10^{-5}$ | 189 | 231 | 400 | 377 | 0.5 | 15.2 | 19.2 |
| RC14 | 500 | $10^{-5}$ | 213 | 225 | 387 | 366 | 0.6 | 19.6 | 24.4 |
| RC10 | 600 | $10^{-1}$ | 207 | 222 | 351 | 336 | 0.4 | 13.3 | 20.0 |
| RC06 | 600 | $10^{-3}$ | 191 | 233 | 384 | 364 | 0.8 | 16.1 | 21.1 |
| RC15 | 600 | $10^{-5}$ | 275 | 275 | 455 | 404 | — | 15.0 | 21.2 |
| RD25 | 700 | $10^{-1}$ | 177 | 214 | 340 | 325 | 0.8 | 14.8 | 21.0 |
| RD14 | 700 | $10^{-3}$ | — | 222 | 388 | 364 | 0.7 | 12.3 | 18.8 |
| RD15 | 700 | $10^{-5}$ | — | 227 | 409 | 397 | 1.0 | 12.7 | 22.3 |
| RD26 | 750 | $10^{-1}$ | 200 | 215 | 338 | 326 | 0.7 | 12.0 | 19.0 |
| RD02 | 750 | $10^{-3}$ | 236 | 243 | 396 | 387 | 0.7 | 10.0 | 16.0 |
| RD17 | 750 | $10^{-5}$ | 200 | 225 | 353 | 353 | 0.8 | 10.8 | 25.5 |
| RD27 | 800 | $10^{-1}$ | 218 | 224 | 331 | 322 | 0.7 | 11.7 | 19.7 |
| RD06 | 800 | $10^{-3}$ | 242 | 234 | 337 | 334 | 0.9 | 11.0 | 19.0 |
| RD18 | 800 | $10^{-5}$ | 185 | 210 | 280 | — | 0.3 | 6.7 | 31.1 |

*Ann. 1150°C, 1h

~$2 \times 10^{-7}$ torr using a screw-driven machine. Specimens were held at test temperature for 20-30 minutes before starting the test. Data were acquired digitally at a rate of 20 points per second.

Results

Testing was carried out at 20, 300, 300, 400, 500, 600, 700, 750, and 800°C at five strain rates between $10^{-1}$ and $10^{-5}$. These data are summarized in Table 1. The main features of the engineering stress-strain curves for V-4Cr-4Ti are shown in Fig. 1, which contains data for nine temperatures obtained at a strain rate of $10^{-3}$/s.

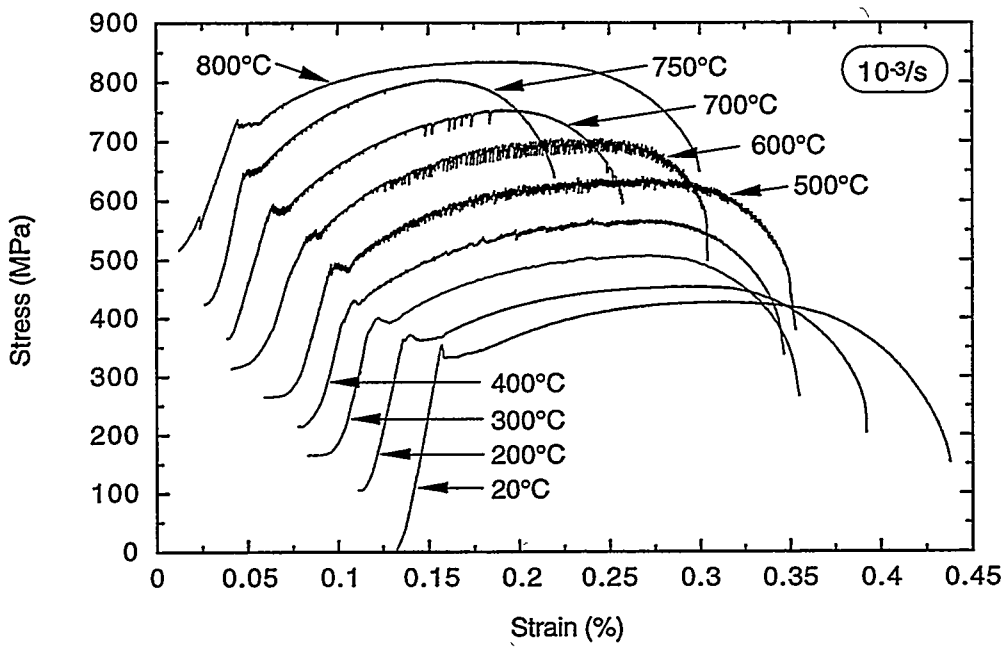


Fig. 1. The stress-strain curves for the V-4Cr-4Ti alloy tested at temperatures between 20 and 800°C.

In the majority of cases, the end of the elastic extension is marked by a small permanent plastic strain of the order of 0.1 to 0.2%. This is followed by a Lüders extension typically ranging from 0.5 to 1.0%. The lower yield stress, $\sigma_y$, is the stress required to propagate the Lüders extension. After the Lüders extension is complete, deformation occurs throughout the specimen on a rising stress-strain curve; eventually the work hardening rate decreases and the ultimate stress, $\sigma_u$, is achieved. For temperatures between 300 and 750°C, the flow curves exhibit jerky flow, which is related to the diffusion of solute atoms to dislocations during the test, i.e. the phenomenon of dynamic strain aging (DSA). As reported earlier [1], both the shape and magnitude of the serrations changes with temperature, strain, and with strain rate; further analysis of this behavior will be presented in future reports.

The strain-rate dependence was determined for the lower yield stress, $\sigma_y$, and for a parameter, $\sigma_s$, which is the stress required to produce a strain of 8% after the completion of the Lüders extension. The 8% strain is an arbitrary value selected to represent material in the strain-hardening regime. The strain-rate sensitivities of these parameters are presented in Figs. 2 and 3.

At 20°C, the lower yield stress exhibits a positive strain rate sensitivity (SRS). The SRS is also positive at 300°C for strain rates $\geq 10^{-3}$/s, however, at lower strain rates, the SRS is markedly less positive (Fig. 2). For temperatures in the range 400 to 800°C, the lower yield point is virtually independent of strain rate over the entire range.

The stress for 8% strain, $\sigma_s$, shows very different behavior (Fig. 3). At 20°C, the SRS is positive over the range $10^{-1}$ to $10^{-4}$/s. At 300°C, however, there is a transition from positive to negative behavior as the strain rate is decreased below ~$10^{-3}$/s. This temperature-dependent transition to a negative SRS coincides with the appearance of jerky flow in the stress-strain curve (Fig. 1).

At 400, 500, 600, and 700°C, the SRS is negative over the full range of strain rates examined with m values in the range (-0.012 to -0.022). All stress strain curves in this regime are characterized by jerky flow behavior with the exception of tests carried out at a rate of $10^{-1}$/s. For these tests, it is possible that the data acquisition system was not sufficiently rapid to detect the load drops; it is planned to repeat these tests with an upgraded, high-speed system.

A different type of behavior was observed at test temperatures of 750 and 800°C. At both temperatures the strain rate sensitivity is negative over the range $10^{-1}$ to $10^{-3}$/s. At lower strain rates, however, m becomes positive, indicating a transition into a different deformation regime.

The temperature-dependence of stress and strain parameters at a strain-rate of $10^{-3}$/s is plotted in Fig. 4.

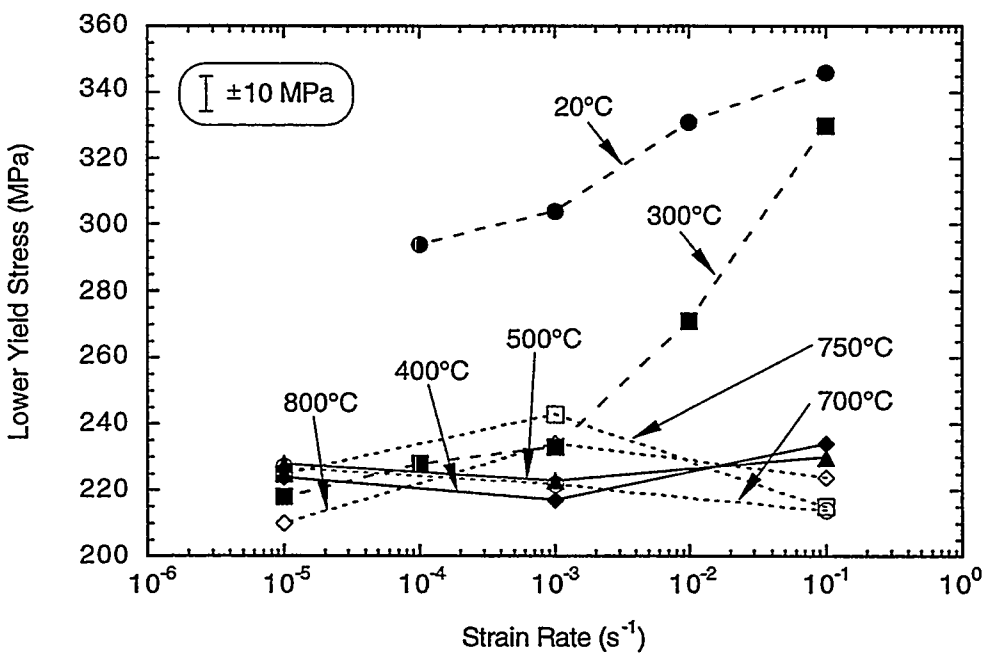


Fig. 2. Effect of strain rate on the lower yield strength of the V-4Cr-4Ti alloy tested at temperatures between 20 and 800°C.

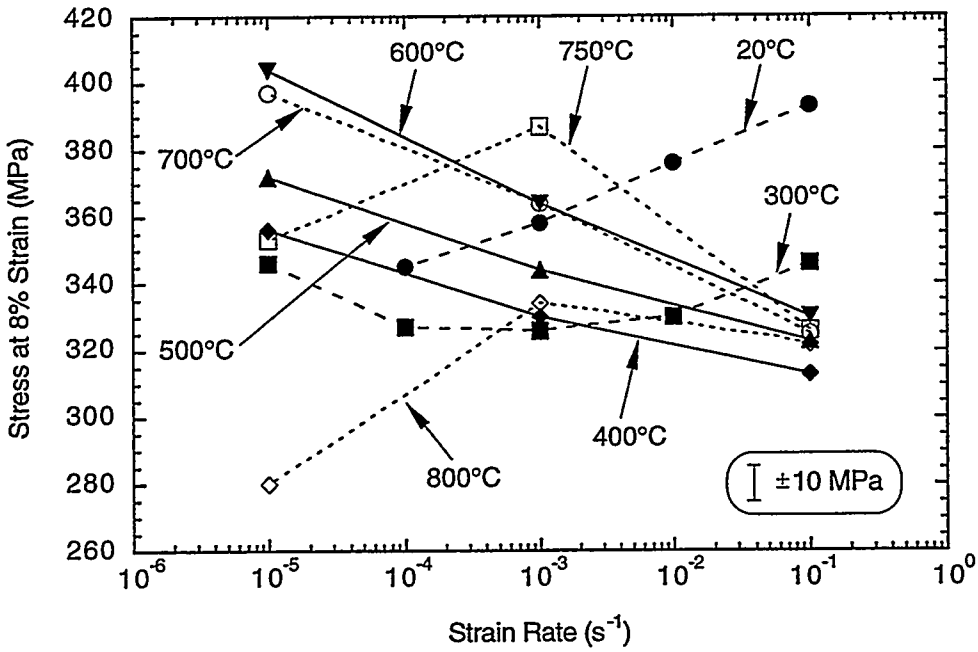


Fig. 3. Effect of strain rate on the tensile strength (measured at 8% strain in the strain-hardening regime) of the V-4Cr-4Ti alloy tested at temperatures between 20 and 800°C.

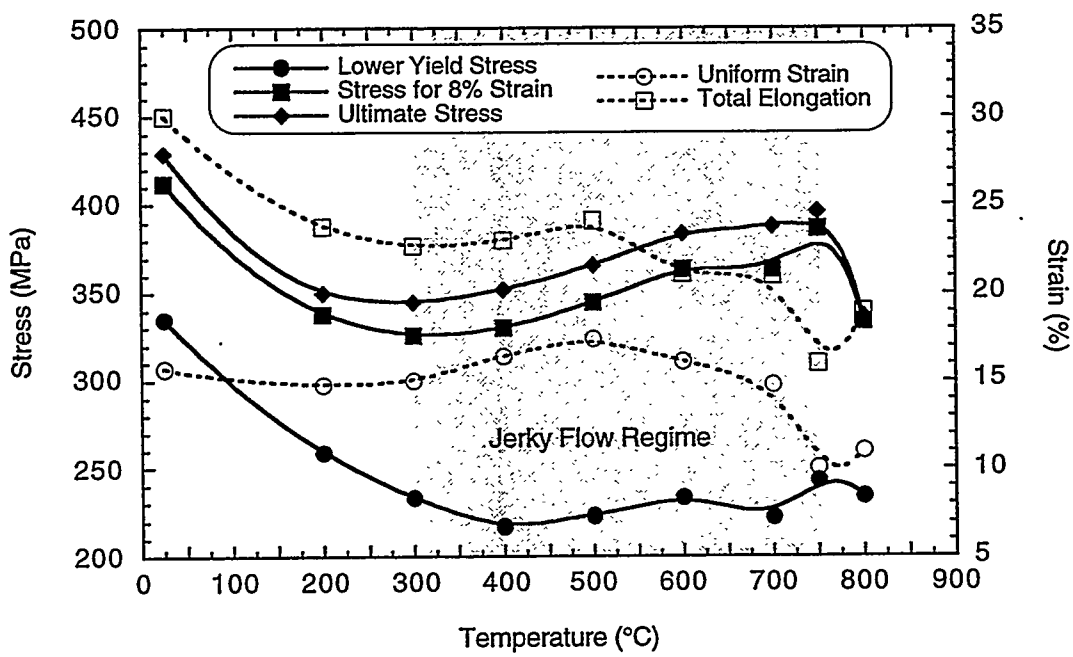


Fig. 4. The temperature-dependence of stress and strain parameters of the V-4Cr-4Ti alloy tested at a strain rate of $10^{-3}$/s.

Discussion

The phenomenon of strain aging occurs in a wide range of FCC, BCC, and HCP alloys (for reviews see references [7, 8]). Strain aging is related to the segregation of mobile solute atoms to temporarily arrested dislocations, which partially impedes dislocation motion. Both substitutional and interstitial solutes can be involved. This pinning of dislocations by solute atmospheres gives rise to the yield point phenomenon that occurs over a broad temperature range. After reaching a peak, the flow stress drops to a lower value as a Lüders deformation front propagates along the specimen gage length at a constant stress. At temperatures where solutes are mobile, the phenomenon of dynamic strain aging (DSA) may occur in which diffusion of solutes to dislocation occurs during straining. The local solute concentration at arrested dislocations, $C_s$, is a function of the waiting time at obstacles $t_w$. When the strain rate is increased, a decrease in flow stress occurs due to a decrease in $C_s$ resulting from the decrease in $t_w$. Thus, the regime of DSA, which is bounded by certain values of temperature and strain rate, is characterized by negative values of the strain rate sensitivity parameter defined by equation (1) above.

The DSA phenomenon gives rise to changes in the appearance of the flow curves. In BCC materials containing interstitial solutes, regular serrations occur in the region of the Lüders extension in the temperature range where interstitials are mobile; this "serrated yielding" occurs at a constant average stress. As the applied stress is increased and the material enters the work hardening regime, the flow curve is characterized by small serrations whose frequency and magnitude vary with strain, temperature and strain-rate. This is the regime of "jerky flow." The ability to detect the upper yield point, serrated yielding, and jerky flow depends upon the sensitivity of the test machine and upon specimen geometry. Detection of serrations is favored by: (a) the use of a "hard" machine, in which a small specimen extension produces a large drop in load, and (b) by a high speed digital data acquisition system. Detection of the upper yield and the observed magnitude of the load drop is sensitive to the specimen geometry, specimen alignment, and surface quality.

Early work by Bradford and Carlson [9] related strain-aging phenomena in pure vanadium at 150-170°C to the diffusion of oxygen and carbon. Subsequently, Thompson and Carlson [10], also working with pure vanadium, were able to relate strain-aging peak over the range 300 to 450°C to the diffusion of nitrogen. In the V-4Cr-4Ti alloy it is expected that a positive interaction between the substitutional titanium atom and the interstitial species [11], will shift the appearance of DSA phenomena to somewhat higher temperatures in the alloy.

The data for the lower yield stress, $\sigma_y$, and for the stress at 8% strain, $\sigma_s$, shown in Figs. 2 and 3 represent deformation in two quite different deformation regimes, and consequently, exhibit rather different strain rate sensitivities. During the Lüders extension, weakly pinned dislocations are activated and slip bands form on only a limited set of available slip planes. Once the Lüders front has propagated along the gage length, the stress must be increased to unlock further dislocations; the dislocation density increases rapidly as the material enters the strain-hardening regime. At room temperature, the SRS of $\sigma_y$ is positive with $m \approx 0.025$. At 300°C, m is positive only for strain rates $\geq 10^{-3}$/s, and for these conditions, serrated yielding in the Lüders regime could not be detected. At lower strain rates, m becomes markedly less positive and serrations begin to appear in the Lüders extension. At all test temperatures above 300°C, although serrated yielding occurs within the Lüders extension for all strain rates, $\sigma_y$ is essentially insensitive to strain rate.

The $\sigma_s$ parameter is measured at a fixed value of the strain (8%), which is well into the strain-hardening regime. At room temperature, the SRS of $\sigma_s$ is positive, with $m \approx 0.019$ (Fig. 3). At

300°C, the strain rate dependence of $\sigma_s$ displays a classic U-shape, with a positive sensitivity at high strain rates undergoing a transition to a negative sensitivity for strain rates $\leq 10^{-3}$/s. Based upon the relative diffusivities of the interstitial species in vanadium, it seems likely that the appearance of jerky flow at low strain rates at 300°C is related to the mobility of carbon and oxygen [1]. At temperatures of 400, 500, 600, and 700°C, the SRS for $\sigma_s$ is always negative, with m in the range (-0.012 to –0.022).

At these temperatures, nitrogen is sufficiently mobile to play a role in DSA. At some temperature, all of the interstitial solutes will be sufficiently mobile to migrate with dislocations moving at the highest strain rates used and will lose their effectiveness in pinning dislocations. It is possible that at sufficiently high temperatures, DSA effects could arise from the substitutional solutes Ti and Cr.

It can be seen from Fig. 1 that the appearance of serrated yielding in the Lüders extension coincides with the appearance of jerky flow in the strain hardening regime, suggesting that the load-drops have a common origin in the locking of dislocations by mobile interstitial species. This type of behavior has been observed in mild steel [12].

The strain rate insensitivity of $\sigma_y$ in the 400 to 700°C range contrasts with the strong negative strain rate sensitivity of $\sigma_s$ over the same range; this difference is not understood at present.

At 750 and 800°C, the negative SRS of $\sigma_s$ for strain rates in the range $10^{-1}$ to $10^{-3}$/s is similar to that for lower temperatures with m in the range (-0.037 to -0.008). At lower strain rates, however, m becomes positive. This reversal in SRS indicates a change in deformation mode and is probably related to a transition into a power law creep regime. Additional intermediate strain rate tests are in progress to allow determination of an activation energy for deformation in this regime. The stress-strain curves at 750°C are compared for two strain rates in Fig. 5. The two curves are very similar,

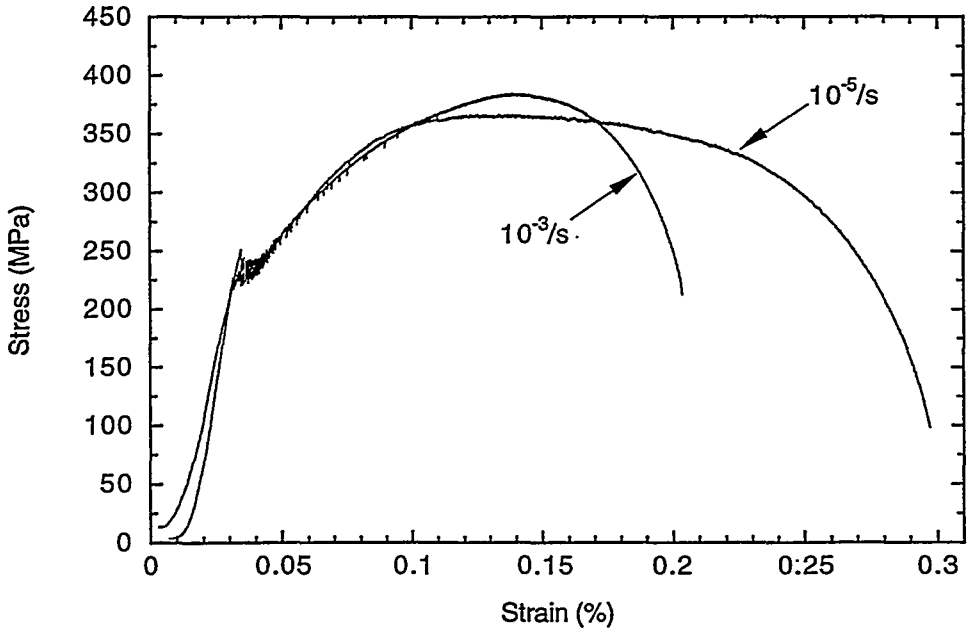


Fig. 5. The stress-strain curves for the V-4Cr-4Ti alloy tested at 750°C and strain rates of $10^{-3}$/s and $10^{-5}$/s.

initially. However, at a strain-rate of $10^{-5}$/s, the strain-hardening rate decreases more rapidly due to climb-enhanced dislocation rearrangement.

Work is continuing to determine the strain rate sensitivity of V-4Cr-4Ti, pure V, and V-4Cr-4Ti weld metal and is also being carried out utilizing hardness and resistivity measurements. Together, these studies will provide the basic information needed to advance our understanding of the effects of test temperature, strain rate, and irradiation on the flow and fracture of V-Cr-Ti alloys.

## REFERENCES


1. A. N. Gubbi, A. F. Rowcliffe, W. S. Eatherly, and L. T. Gibson, "Effects of Strain Rate, Test Temperature, and Environment on the Tensile Properties of Vanadium Alloys," Fusion Materials Semiannual Progress Report, DOE/ER-0313/20, June 1996, p. 38.

2. S. A. Bradford and O. N. Carlson, Trans. AIME **224** (1962), pp. 738-742.

3. S. J. Zinkle, L. L. Snead, J. P. Robertson, and A. F. Rowcliffe, "Strain Rate Dependence of the Tensile Properties of V-4Cr-4Ti Irradiated in EBR-II and HFBR," Fusion Materials Semiannual Progress Report, DOE/ER-0313/23, December 1997, p. 77.

4. S. J. Zinkle, L. L. Snead, A. F. Rowcliffe, D. J. Alexander, and L. T. Gibson, "Effects of Irradiation Temperature and Strain Rate on the Mechanical Properties of V-4Cr-4Ti Irradiated to Low Doses in Fission Reactors," Fusion Materials Semiannual Progress Report, DOE/ER-0313/24, June 1998, p. 33.

5. S. J. Zinkle, A. F. Rowcliffe, and C. O. Stevens, "High Temperature Tensile Properties of V-4Cr-4Ti," Fusion Materials Semiannual Progress Report, DOE/ER-0313/24, June 1998, p. 11.

6. A. F. Rowcliffe and D. T. Hoelzer, "Microstructural Inhomogeneities in V-4Cr-4Ti Mechanical Property Specimens Prepared for Irradiation Experiments in HFBR, BOR-60, and HFIR," Fusion Materials Semiannual Progress Report, DOE/ER-0313/25, December 1998, p. 42.

7. B. J. Brindley and P. J. Worthington, "Yield-Point Phenomena in Substitutional Alloys," Metallurgical Reviews 15, 101, 1970.

8. J. D. Baird, Metallurgical Reviews 5, 1-18, 1971.

9. S. A. Bradford and O. N. Carlson, "The Role of Oxygen in Strain-Aging of Vanadium," Trans AIME 224, Aug. 1962, p. 738

10. R. W. Thompson and O. N. Carlson, "Strain-Aging Effects of Nitrogen in Vanadium, J. Less Common Metals 7, 1964, p. 321.

11. T. Shikama, S. Ishino, and Y. Mishima, "The Interaction Between Interstitital Impurities and Substitutional Solutes in Vanadium," J. Nucl. Mats 68, 1977, p. 315.

12. Y. Bergström and W. Roberts, Acta Met. 19, 815-823, 1971.